


## 2-Naphthol scaffold as selective colorimetric and fluorescence 'turn-on' sensor of $\text{PO}_4^{3-}$

Naren Mudi, Prabhat Kr. Giri, Shashanka Shekhar Samanta, Usha Mandal, Rodrigo Ramirez Tagle & Ajay Misra



To cite this article: Naren Mudi, Prabhat Kr. Giri, Shashanka Shekhar Samanta, Usha Mandal, Rodrigo Ramirez Tagle & Ajay Misra (2023): 2-Naphthol scaffold as selective colorimetric and fluorescence 'turn-on' sensor of  $\text{PO}_4^{3-}$ , International Journal of Environmental Analytical Chemistry, DOI: [10.1080/03067319.2023.2221194](https://doi.org/10.1080/03067319.2023.2221194)

To link to this article: <https://doi.org/10.1080/03067319.2023.2221194>

 View supplementary material 

 Published online: 07 Jun 2023.

 Submit your article to this journal 

 View related articles 

 View Crossmark data 



## 2-Naphthol scaffold as selective colorimetric and fluorescence 'turn-on' sensor of $\text{PO}_4^{3-}$

Naren Mudi<sup>a</sup>, Prabhat Kr. Giri<sup>a</sup>, Shashanka Shekhar Samanta<sup>a</sup>, Usha Mandal<sup>a</sup>,  
Rodrigo Ramirez Tagle<sup>b</sup> and Ajay Misra<sup>a</sup>

<sup>a</sup>Department of Chemistry, Vidyasagar University, Midnapore, India; <sup>b</sup>Universidad de las Americas, Santiago, Chile

### ABSTRACT

1-(Pyridin-2-yl-hydrazonomethyl)-naphthalen-2-ol (PNOH) is a naphthalene-based fluorescence chemo-sensor for  $\text{PO}_4^{3-}$ . The probe (PNOH) is spectroscopically characterised and the chemosensing mechanism has been demonstrated through  $^1\text{H}$  NMR, UV-Vis absorption and both steady-state and time resolved fluorescence study. Fluorescence 'turn-on' sensing knack of PNOH towards  $\text{PO}_4^{3-}$  ion has been explained due to emission from the excited  $\text{PNO}^-$  ion, formed upon transfer of phenolic proton of PNOH to  $\text{PO}_4^{3-}$  ion in the excited state. The 1:1 stoichiometry of PNOH- $\text{PO}_4^{3-}$  complex is observed from Job's plot based on UV-Vis titration and the complex shows distinct yellowish-green colour to be used as colorimetric sensor for  $\text{PO}_4^{3-}$ . Limit of detection (LOD) of PNOH towards  $\text{PO}_4^{3-}$  is found to be  $0.35\ \mu\text{M}$ . It is also demonstrated that the probe can be used to fabricate a convenient and efficient  $\text{PO}_4^{3-}$  paper test kits as well as molecular INHIBIT logic gate.

### ARTICLE HISTORY

Received 15 January 2023  
Accepted 26 May 2023

### KEYWORDS


PNOH;  $\text{PO}_4^{3-}$  sensor; INHIBIT logic gate; paper strip

## 1. Introduction

Roles of anions in biological, environmental and medicinal chemistry are very important [1–6]. Among the anions, phosphate ( $\text{PO}_4^{3-}$ ) ion is an essential part of nucleotides, which leads to many crucial functions in cellular signalling, energy storage, bone mineralisation, muscle function and other fundamental biological processes [7–9]. Excessive presence of  $\text{PO}_4^{3-}$  in environment can disrupt aquatic life cycle [10] and also leading to many health problems [11]. Therefore, the designing of a new chemosensor is highly demanding to monitor  $\text{PO}_4^{3-}$  ion with high degree of sensitivity and selectivity.

Detection of  $\text{PO}_4^{3-}$ , colorimetrically as well as fluorometrically is categorised in two different types among the reported  $\text{PO}_4^{3-}$  sensors. (i) Based on metal complex probe where the presence of unsaturated coordination sphere of metal can bind the target anion and follow emission quenching (turn-off) [12,13] or emission enhancing (turn-on) [14,15] mechanism. (ii) Based on tetraphenylethylene (TPE) core ligands [16,17] where mainly charge-transfer or H-bonding interaction occurred with anion. Disadvantages of

**CONTACT** Ajay Misra ✉ [ajay@mail.vidyasagar.ac.in](mailto:ajay@mail.vidyasagar.ac.in)

 Supplemental data for this article can be accessed online at <https://doi.org/10.1080/03067319.2023.2221194>.

© 2023 Informa UK Limited, trading as Taylor & Francis Group

these type sensors are their poor selectivity and having hazardous multi-step synthetic procedure.

In extension to our foregoing reports [18], we have used the naphthalene-based probe, 1-(pyridin-2-yl-hydrazonomethyl)-naphthalen-2-ol (PNOH) as a turn-on fluorescence chemosensor for the selective detection  $\text{PO}_4^{3-}$  ion in water sample. The phenolic ( $-\text{OH}$ ) proton and amine ( $\text{N-H}$ ) proton of PNOH give an opportunity of H-bond donor and also interaction with methane ( $\text{C-H}$ ) proton [19] towards anion. PNOH itself has non-planar structure and very weakly fluorescent due to various non-radiative modes e.g. intramolecular rotation, large amplitude vibrational modes which facilitates the non-radiative decay pathways. It is observed that PNOH selectively binds with  $\text{PO}_4^{3-}$  ion and the complex shows 'turn on' emission property due to excited state proton transfer from phenolic  $-\text{OH}$  to the  $\text{PO}_4^{3-}$  ion. Interestingly, PNOH shows selective colorimetric and fluorometric sensing towards  $\text{PO}_4^{3-}$  ion even in the presence of other phosphate e.g.  $\text{HPO}_4^{2-}$  and  $\text{H}_2\text{PO}_4^-$  ions. Paper strip kits to detect  $\text{PO}_4^{3-}$  ion in real water sample have been demonstrated. Further, fluorescence 'turn on' and 'turn off' behaviour of PNOH in presence of  $\text{PO}_4^{3-}$  ions and  $\text{H}^+$  ions respectively have been used to fabricate molecular INHIBIT logic gate.

## 2. Experimental section

### 2.1. Materials and instrumentations

Synthesis of PNOH from 2-hydroxy-1-naphthaldehyde and 2-hydrazinopyridine had been reported previously by our group [18]. Sodium salt of all anions was purchased from SRL pvt. Ltd., India. Spectroscopic grade Ethanol and DMSO were received from Spectrochem pvt. Ltd., India, and freshly prepared double-distilled deionised water was used throughout the experiment. UV-Vis absorption and steady-state emission spectra were recorded on a Shimadzu UV 1800 spectrophotometer and HITACHI (Model no. F-7001) fluorescence spectrometer, respectively. NMR study of the samples was carried out on Bruker ASCEND 400 MHz spectrometer using  $\text{DMSO-d}_6$  as solvent. Elemental analyses were performed on a Perkin Elmer 2400 CHN analyser. Time correlated single photon counting (TCSPC) set up from Horiba Jobin-Yvon (Delta Flex) was used to perform fluorescence lifetime measurements. Nano-LED of 416 nm was used as the excitation source. The fluorescence decay data were analysed using IBH DAS 6 software.

### 2.2. Sample preparation for UV-Vis and fluorescence spectral studies

A stock solution of PNOH (40  $\mu\text{M}$ ) was prepared in DMSO and the solution was used for UV-Vis and fluorescence measurements. Stock solutions (1.0 mM) of sodium salts of different anions ( $\text{F}^-$ ,  $\text{Cl}^-$ ,  $\text{Br}^-$ ,  $\text{CN}^-$ ,  $\text{OAc}^-$ ,  $\text{HAsO}_4^-$ ,  $\text{N}_3^-$ ,  $\text{AsO}_4^{3-}$ ,  $\text{I}^-$ ,  $\text{HPO}_4^{2-}$ ,  $\text{SO}_4^{2-}$ ,  $\text{NO}_3^-$ ,  $\text{H}_2\text{PO}_4^-$ ,  $\text{S}_2\text{O}_4^{2-}$ ,  $\text{SCN}^-$ ,  $\text{HSO}_4^-$ ,  $\text{HSO}_3^-$ ) were prepared in doubly distilled deionised water. Freshly prepared standard solutions of anions (1.0 mM in deionised water) were added with increasing concentrations in a 3 ml solution of PNOH (40  $\mu\text{M}$ ) to record the UV-Vis and fluorescence spectra. Fluorescence measurements of all the samples were carried out with 420 nm excitation. All fluorescence and absorbance spectra were recorded instantly after the addition of each anion to PNOH solution.

### 2.3. Detection limit

The detection limit was calculated using fluorescence titration data of PNOH vs  $\text{PO}_4^{3-}$ . The fluorescence intensity (at 505 nm) of PNOH as a function of its increasing concentration was measured and the standard deviation ( $\sigma$ ) of blank measurement was calculated. To obtain the slope ( $k$ ), the fluorescence emission intensity at 505 nm was plotted against the increasing concentration of  $\text{PO}_4^{3-}$ . Detection limit of the probe for sensing  $\text{PO}_4^{3-}$  was calculated using  $3\sigma$  method [20].

$$\text{Detection limit} = 3\sigma/k.$$

LOD for colorimetric measurement was carried out using the above method ( $3\sigma/k$ ) and the UV-Vis absorption at 375 nm was used for both the measurement of standard deviation ( $\sigma$ ) and the slope ( $k$ ).

## 3. Results and discussion

### 3.1. Analytical sensing of PNOH towards $\text{PO}_4^{3-}$

#### 3.1.1. UV-Vis absorption & NMR titration

UV-Vis absorption spectra were recorded upon addition of two equivalent of sodium salt (80  $\mu\text{M}$ ) of each anions to PNOH (40  $\mu\text{M}$ ) in DMSO separately and the volume percentage ratio of DMSO: water is 93:7 in each study (Figure 1a). Except  $\text{PO}_4^{3-}$  ion, no significant change in the absorption spectra were observed after the addition of anion solution to PNOH

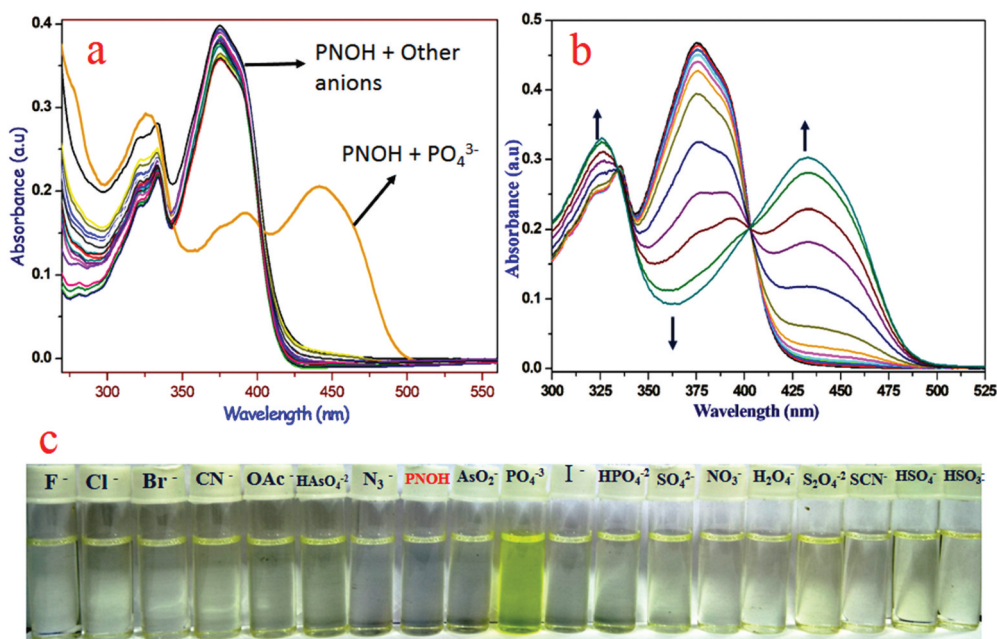


**Figure 1.** (a) Absorption spectra of PNOH (40  $\mu\text{M}$  in DMSO) in the presence of various anions (80  $\mu\text{M}$  in water), (b) absorption spectra of PNOH (40  $\mu\text{M}$  in DMSO) with gradual addition of  $\text{PO}_4^{3-}$  (0–80  $\mu\text{M}$  in water), (c) images of samples containing PNOH (40  $\mu\text{M}$  in DMSO) and sodium salts of various anions (80  $\mu\text{M}$  in DMSO) under day light. Volume percentage ratio of DMSO/water is 93/7.

(Figure 1a). UV-Vis absorption spectra of PNOH in the presence of increasing concentration of  $\text{PO}_4^{3-}$  ion show the appearance of a red shifted broad band with maxima at 432 nm and a clear isosbestic point at 401 nm (Figure 1b). This red shifted band has been assigned to the complex formed between PNOH and

$\text{PO}_4^{3-}$  ion. Since  $\text{PO}_4^{3-}$  ion is basic in nature, UV-Vis absorption study of PNOH in the presence of a strong base NaOH was carried out. UV-Vis spectra of PNOH show a distinct red shifted ( $\lambda_{\text{max}} = 452$  nm) broad absorption band in the presence of NaOH (Figure S1a). It is also observed that the characteristic band of PNOH at  $\lambda_{\text{max}} = 375$  nm decreases and the red shifted band ( $\lambda_{\text{max}} = 452$  nm) increases with a clear isosbestic point at 401 nm with the increasing concentration of NaOH. Again, the proton NMR spectra (Figure S2) of PNOH in the presence of alkali (NaOD) show the complete disappearance of -OH proton ( $\delta = 12.00$  ppm). But the  $^1\text{H}$  NMR spectra of PNOH in the presence of  $\text{PO}_4^{3-}$  ion shows upfield shift of all the O-H (a), N-H (b) and =C-H (c) protons due to strong shielding of  $\text{PO}_4^{3-}$  ion (Figure S3). The above  $^1\text{H}$  NMR data reveal that phenolic proton of PNOH is in close proximity with  $\text{PO}_4^{3-}$ . Thus, the red shifted band at 452 nm is due to  $\text{PNO}^-$  ion in the solution. Similar red shifted band ( $\lambda_{\text{max}} = 432$  nm) of PNOH in the presence of  $\text{PO}_4^{3-}$  indicates that the phenolic -OH group is one step forward to be detached from PNOH. Our DFT-based computational study also reveals that the electronic transition energy of  $\text{PNO}^-$  ion (3.340 eV) is much lower than PNOH (3.690 eV) and the computed values nicely corroborate with the experimental absorption maxima [18].

Stoichiometry in the ground state complexation between PNOH and  $\text{PO}_4^{3-}$  is calculated from the Job's plot (Figure S4) and it is found to be 1:1. Thus, PNOH acts as a selective colorimetric sensor of  $\text{PO}_4^{3-}$  ion by changing its colour from very faint yellow to yellowish-green (Figure 1c) and this visible change of colour can be detected even in naked eye. Limit of detection (LOD) of probe PNOH towards  $\text{PO}_4^{3-}$  ion has been calculated using UV-Vis titration data (Figure S5) and the observed LOD value is 16.17  $\mu\text{M}$ .

The selective sensing mechanism of  $\text{PO}_4^{3-}$  was also investigated through  $^1\text{H}$  NMR titration in  $\text{DMSO-}D_6$ . Initially sensor, PNOH shows peaks in the region 6.82–8.37 ppm for 10 aromatic protons and the three single proton peaks assigned for -OH (marked 'a'), -NH- (marked 'b') and =CH- (marked 'c') are at 12.00 ppm, 11.03 ppm and 9.10 ppm, respectively (Figure S3A). There is an overall upfield shift for proton-a ( $\Delta = 3.41$  ppm), proton-b ( $\Delta = 2.89$  ppm), proton-c ( $\Delta = 0.3$  ppm) and aromatic protons (6.60–7.62 ppm) after the addition of one equivalent  $\text{PO}_4^{3-}$  anion to PNOH (Figure S3B). This up field shift of protons may be attributed to high electron density induced shielding of  $\text{PO}_4^{3-}$  anion present in PNOH- $\text{PO}_4^{3-}$  complex. Addition of higher concentration (>1 eqv.) of  $\text{PO}_4^{3-}$  shows almost no change of chemical shift of protons (Figure S3C) compare to the addition of one equivalent  $\text{PO}_4^{3-}$  to PNOH. Thus, proton NMR spectra of PNOH in the presence of  $\text{PO}_4^{3-}$  ion support the 1:1 stoichiometry of PNOH:  $\text{PO}_4^{3-}$  in PNOH- $\text{PO}_4^{3-}$  complex.

### 3.1.2. Steady state and time resolved emission study

Steady-state fluorescence study of PNOH (40  $\mu\text{M}$  in DMSO) in the presence of all the studied anions except  $\text{PO}_4^{3-}$  ion show quenching in emission. Addition of  $\text{PO}_4^{3-}$  to PNOH displays broad red-shifted 'turn-on' green emission with peak at 502 nm (Figure 2a) as compare to PNOH. Incremental addition of  $\text{PO}_4^{3-}$  to PNOH shows gradual increase of fluorescence intensity (Figure 2b) upon excitation at 420 nm.

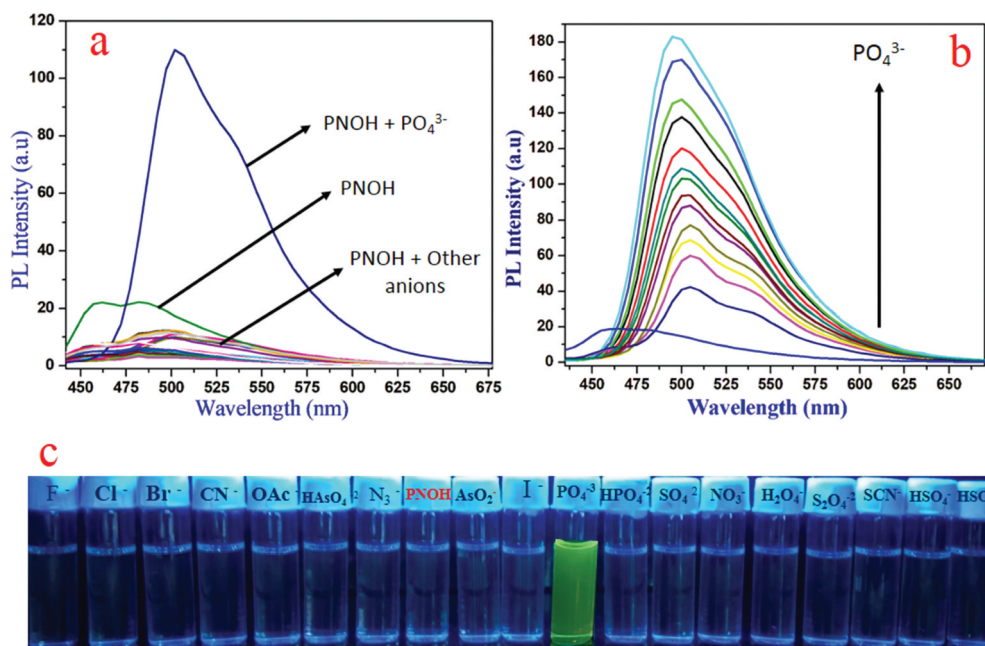


**Figure 2.** (a) Fluorescence emission spectra of PNOH (40  $\mu\text{M}$  in DMSO) in the presence aqueous of various anions (80  $\mu\text{M}$ );  $\lambda_{\text{ex}} = 420 \text{ nm}$ , (c) fluorescence emission spectra of PNOH (40  $\mu\text{M}$  in DMSO) with incremental addition (0–80  $\mu\text{M}$ ) of aqueous solution of  $\text{PO}_4^{3-}$  in water;  $\lambda_{\text{ex}} = 420 \text{ nm}$ , (b) images of samples containing PNOH (40  $\mu\text{M}$  in DMSO) and sodium salts of various anions (80  $\mu\text{M}$  in water) under the irradiation of 365 nm light. Volume percentage of DMSO/water is 93/7.

$\text{PO}_4^{3-}$  ion is a hard base and it can easily accept the phenolic proton of excited PNOH due to its close proximity in PNOH-  $\text{PO}_4^{3-}$  complex. In order to substantiate the origin of fluorescence, a controlled fluorescence study of PNOH in the presence of strong base NaOH has been carried out (Figure S1b). Figure S1b shows a broad red shifted emission with emission maxima at 502 nm and the intensity of 502 nm band increase with the increasing concentration of NaOH. Thus, the observed emission of PNOH in the presence of  $\text{PO}_4^{3-}$  ion (Figure 2b) is identical to that of PNOH in the presence of base, NaOH. The strong base NaOH can easily deprotonate the phenolic proton of PNOH to form  $\text{PNO}^-$  and the strong emission at 502 nm is due to the excited  $\text{PNO}^-$ . Our UV-Vis and  $^1\text{H}$  NMR study show the existence of PNOH-  $\text{PO}_4^{3-}$  complex where  $\text{PO}_4^{3-}$  ion is closely attached with the phenolic proton of PNOH. It is well known that the  $pK_a$  value of enol proton decreases in the excited singlet state [21]. Thus, the closely attached  $\text{PO}_4^{3-}$  ion can easily deprotonate the phenolic proton to form  $\text{PNO}^-$  ion in the excited state. This excited  $\text{PNO}^-$  ion shows the intense emission at 502 nm during the fluorescence emission study of PNOH in the presence of  $\text{PO}_4^{3-}$  ion.

Comparative study for onsite detection of  $\text{PO}_4^{3-}$  anion has been carried out through visual colour change from colourless to light green under UV-light (Figure 2c). Fluorescence quantum yield of PNOH was calculated in the absence and presence of phosphate ion using quinine sulphate as the standard [22], and it was observed that the

**Table 1.** Average fluorescence lifetime, quantum yield, radiative and non-radiative rate constants of PNOH, PNOH in the presence of  $\text{PO}_4^{3-}$  and PNOH with NaOH. Volume percentage of DMSO to water is 93:7 in each study.

Species	$\tau_f$ (avg. ns)	Quantum Yield ( $\Phi_f$ )	$K_r$ ( $\text{S}^{-1}$ ) ( $\Phi_f/\tau_f$ ) $\times 10^9$	$K_{nr}$ ( $\text{S}^{-1}$ ) [[ $1/\tau_f$ ]- $K_r$ ] $\times 10^9$	$\chi^2$
PNOH	0.76	0.001	0.0013	1.13	0.96
(PNOH + $\text{PO}_4^{3-}$ ) -Complex	2.4	0.012	0.005	0.41	0.97
PNOH + NaOH	2.3	0.013	0.005	0.40	1.01

fluorescence quantum yield (Table 1) of PNOH in the presence of phosphate ion ( $\Phi = 0.012$ ) increases to  $\sim 12$  times than that of only PNOH ( $\Phi = 0.001$ ).

To explore the ‘turn-on’ mechanism of  $\text{PO}_4^{3-}$ , we further performed time resolved photoluminescence (TRPL) experiment (Figure 3). Average fluorescence lifetime of PNOH is 0.76 ns and that of PNOH in the presence of  $\text{PO}_4^{3-}$  ion is 2.4 ns. In accordance with the steady-state fluorescence, we also carried out the fluorescence lifetime measurements of PNOH in the presence of strong base NaOH (Table 1). The measured fluorescence lifetime (2.3 ns) is identical to that of PNOH in the presence of  $\text{PO}_4^{3-}$  ion. Quantum yield ( $\Phi_f$ ), radiative ( $K_r$ ) and non-radiative ( $K_{nr}$ ) rate constant of PNOH, PNOH in the presence of  $\text{PO}_4^{3-}$  ion and PNOH in the presence of strong base NaOH were calculated from the fluorescence quantum yield and fluorescence lifetime data and are presented in Table 1. All these values as shown in Table 1 are almost similar in case of PNOH in the presence of

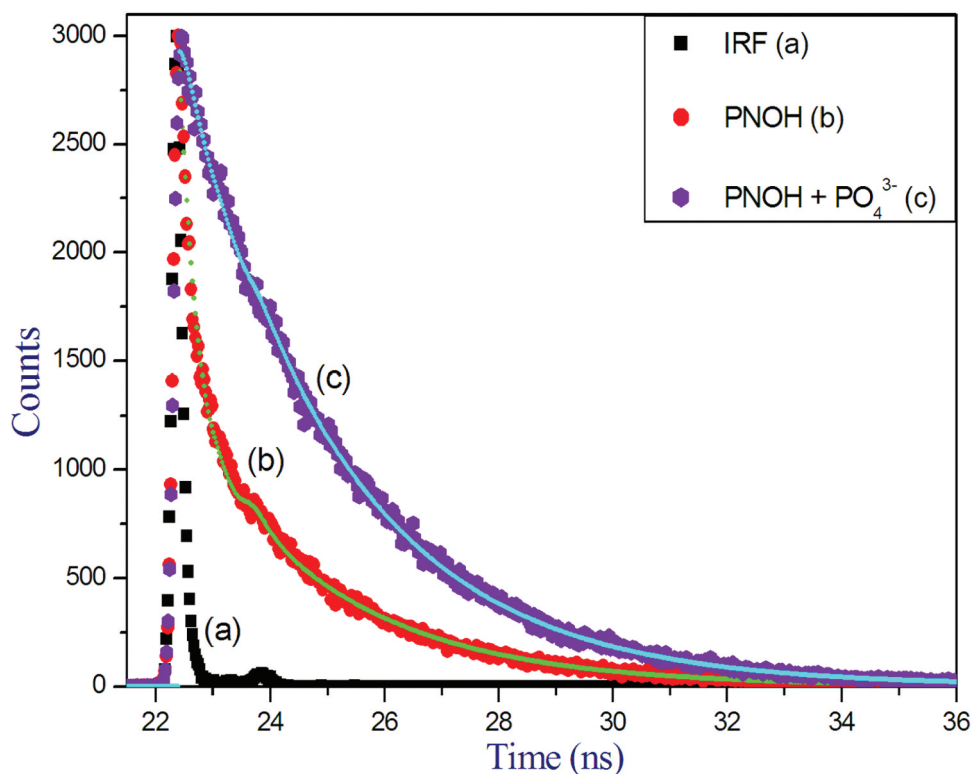


**Figure 3.** Fluorescence decay profile of (a) IRF (b) PNOH and (c) PNOH in presence of  $\text{PO}_4^{3-}$ .

$\text{PO}_4^{3-}$  ion and PNOH in the presence of NaOH and the values are differed significantly compare to the only PNOH in the solution. High values of both quantum yield and radiative rate constant PNOH in the presence of  $\text{PO}_4^{3-}$  ion are reflected on the 'turn on' emission behaviour of PNOH in the presence of  $\text{PO}_4^{3-}$  ion. Thus, the steady-state and time resolved fluorescence study unequivocally supports that the emitting species is excited  $\text{PNO}^-$  as  $\text{PO}_4^{3-}$  ion is added to PNOH.

### 3.1.3. Selectivity studies

In order to establish the specific selectivity of PNOH towards  $\text{PO}_4^{3-}$ , single and dual anion competitive study was also carried out and is shown in Figure 4. In single anion sensing study,

aqueous solution of two equivalents (80  $\mu\text{M}$ ) of each anion was added to PNOH (40  $\mu\text{M}$ ) in DMSO. Results (Figure 4) show that except  $\text{PO}_4^{3-}$ , other anions do not cause any significant change in fluorescence intensity under the similar conditions, indicating that the selectivity of PNOH towards  $\text{PO}_4^{3-}$  over other anions is remarkably high (blue bars). For the dual-anion competitive studies (green bars), equal amounts of aqueous solutions of  $\text{PO}_4^{3-}$  and other competitive anions (2 eqv. each) were mixed. Fluorescence enhancements were observed in all the cases and the presence of other anions (except  $\text{Cl}^-$  and  $\text{Br}^-$ ) has little effect on the 'turn-on' emission of PNOH in the presence of  $\text{PO}_4^{3-}$  (Figure 4). It clearly indicates the excellent anti-interference performance of PNOH for monitoring phosphate ion ( $\text{PO}_4^{3-}$ ) in the presence of other anions.

### 3.1.4. Detection limit and binding constant

The detection limit was calculated from the fluorescence titration data of PNOH in the presence of  $\text{PO}_4^{3-}$  ion (Figure S6). The standard deviation ( $\sigma$ ) was calculated from the plot of emission intensity ( $\lambda_{\text{max}} = 502 \text{ nm}$ ) as a function of increasing concentration of PNOH in

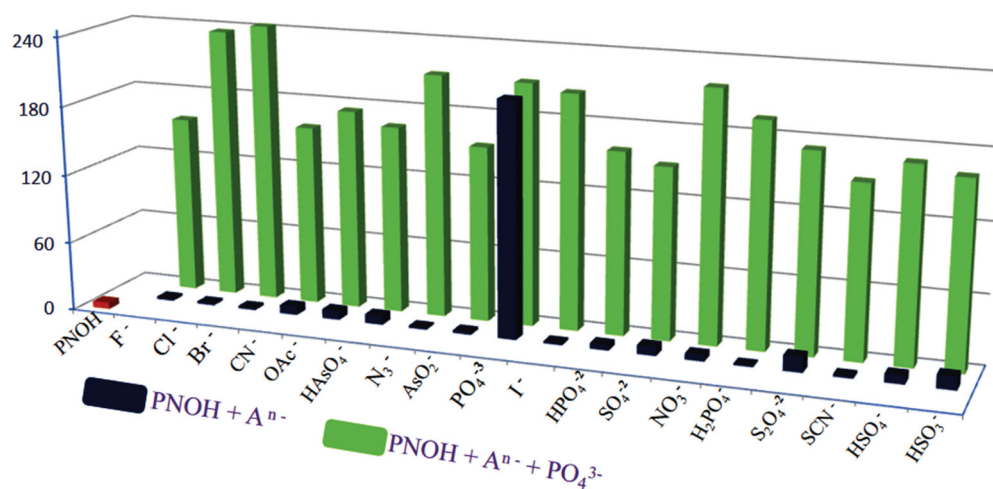


**Figure 4.** Interfering study of other anions towards sensing of  $\text{PO}_4^{3-}$  by PNOH (40  $\mu\text{M}$ ). Blue bars: Single anion competitive study [PNOH (40  $\mu\text{M}$ ) +  $\text{A}^{n-}$  (80  $\mu\text{M}$ )]. Green bars: Dual anion competitive study [PNOH (40  $\mu\text{M}$ ) +  $\text{A}^{n-}$  (80  $\mu\text{M}$ ) +  $\text{PO}_4^{3-}$  (80  $\mu\text{M}$ )]. Here  $\text{A}^{n-}$  indicates various competing anions.  $\lambda_{\text{ex}} = 420 \text{ nm}$ ,  $\lambda_{\text{em}} = 502 \text{ nm}$ . Volume percentage of water and DMSO is 7:93 in each study.



the absence of  $\text{PO}_4^{3-}$  (Figure S6a). On the other hand, the slope ( $k$ ) was obtained from the linear plot of the emission intensity of PNOH with increasing phosphate ion concentration (Figure S6b). From the slope ( $k$ ) and the standard deviation ( $\sigma$ ), the detection limit was estimated using equation,  $\text{LOD} = 3\sigma/k$  and the observed LOD is  $0.35 \mu\text{M}$ . This LOD value is exceptionally low compared to the other reported  $\text{PO}_4^{3-}$  sensors [12,14,15]. Binding constant ( $K_a$ ) of PNOH- $\text{PO}_4^{3-}$  complex was calculated from the fluorescence titration data as a function of concentration of phosphate anion ( $\text{PO}_4^{3-}$ ), using the modified Benesi-Hildebrand equation [23].

$$1/\Delta I = 1/\Delta I_{\max} + \frac{1}{K[C]} (1/\Delta I_{\max})$$

Here  $\Delta I = I - I_{\min}$  and  $\Delta I_{\max} = I_{\max} - I_{\min}$ , where  $I_{\min}$ ,  $I$ , and  $I_{\max}$  are the observed emission intensities of probe PNOH at 502 nm observed in the absence of  $\text{PO}_4^{3-}$  ion, at an intermediate  $\text{PO}_4^{3-}$  ion concentration, and at a concentration of complete saturation of fluorescence intensity, respectively. ' $K$ ' and ' $[C]$ ' are the binding constant and the anion concentration respectively. From the plot of  $1/\Delta I$  vs.  $[C]^{-1}$  for receptor, the value of  $K$  has been determined from the slope. The observed binding constant of PNOH- $\text{PO}_4^{3-}$  complex is  $6.3 \times 10^4 \text{ M}^{-1}$  (Figure S7).

### 3.1.5. Comparative study

Our survey on the  $\text{PO}_4^{3-}$  ion sensor and a comparison with our reported probe is presented in Table S1. All the probe except PNOH as given in Table S1 involve multistep synthesis process. Except the report of Y.S. Zheng et al. [16], all other sensing mechanisms are similar involving the metal ion complexation followed by  $\text{PO}_4^{3-}$  ion sensing. Thus, the direct detection of  $\text{PO}_4^{3-}$  ion using fluorescence technique is not much in the literature. Our synthesised probe PNOH has the edge over the other reported  $\text{PO}_4^{3-}$  ion sensor, since its synthesis involves only a single-step condensation method with high yield of synthesis. Again, the response time, LOD of our synthesised probe ( $0.35 \mu\text{M}$ ) is much lower than the others as given in Table S1. Similar to other reported  $\text{PO}_4^{3-}$  ion sensor, present synthesised probe, PNOH can be used as both fluorometric and colorimetric detection of  $\text{PO}_4^{3-}$  ion.

### 3.1.6. Reversibility study

Reversibility is an important criterion for any chemosensor i.e. reuse of sensor over period of time. The lower pKa value of excited phenolic - OH group of PNOH makes it easily available to any strong proton acceptor like  $\text{PO}_4^{3-}$  ion which is attached to it during ground state complexation. The excited state energy of  $\text{PNO}^-$  is much lower than PNOH and the broad red shifted emission at 502 nm arises from the excited  $\text{PNO}^-$  ion. Now incremental addition of dilute  $\text{H}^+$  ( $0.01 \text{ M}$ ) to the PNOH- $\text{PO}_4^{3-}$  complex solution, decrease the emission intensity of 502 nm band and we continue the addition of  $\text{H}^+$  till the emission intensity reaches its origin value (Figure 5a).

Here,  $\text{PO}_4^{3-}$  anion gets protonated upon gradual addition of  $\text{H}^+$  and no longer available for H-bonding interaction with probe PNOH. Therefore, the probe PNOH becomes free from  $\text{PO}_4^{3-}$  and shows its original reduced emission intensity. Simultaneous addition of  $\text{PO}_4^{3-}$  followed by  $\text{H}^+$  to the PNOH solution were carried out to study reversibility of sensing for a number of cycles. It was observed that even after 9<sup>th</sup> cycles repetition

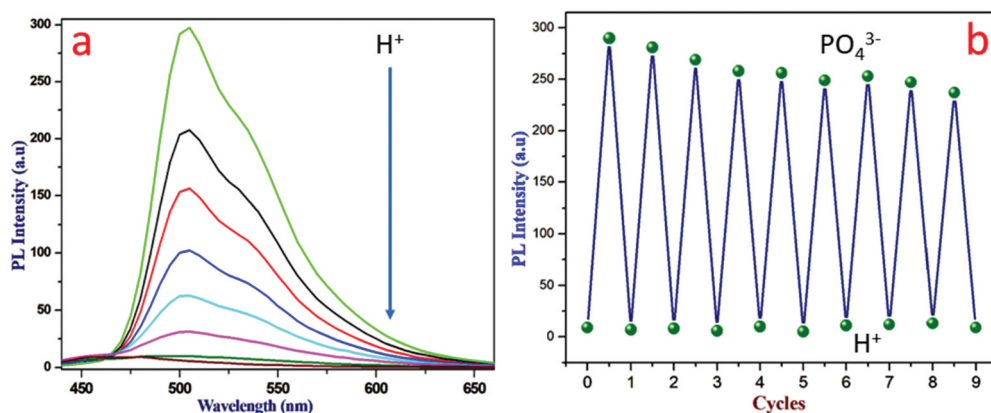


**Figure 5.** (a) Reversibility titration with  $\text{H}^+$  of  $\text{PNOH-PO}_4^{3-}$  complex ( $\lambda_{\text{ex}} = 420 \text{ nm}$ ), (b) Reversibility cycles; ( $\lambda_{\text{ex}} = 420 \text{ nm}$ ,  $\lambda_{\text{em}} = 502 \text{ nm}$ ). Initial volume percentage of water and DMSO is 7:93.

fluorescence intensity did not change much beyond the experimental error limit (Figure 5b).

### 3.2. INHIBIT logic gate

Fluorescence 'turn-on' and 'turn-off' behaviour of PNOH in the presence of  $\text{PO}_4^{3-}$  and  $\text{H}^+$  ion may be used to construct molecular logic gate [24,25]. An INHIBIT logic gate is made of particular combination of the logic operation of AND and NOT functions i.e. output signal is inhibited by only one type of input. Demonstration of INHIBIT logic gate is shown in Figure 6.

$\text{H}^+$  can effectively free the probe PNOH from its anion complex ( $\text{PNOH-PO}_4^{3-}$ ) and hinder the formation of  $\text{PNO}^-$  ion in the excited state. Thus, the emission is turned off (Figure 6). However, in the absence of  $\text{PO}_4^{3-}$ ,  $\text{H}^+$  has little effect on the emission intensity of PNOH at 502 nm. Thus, logic gate can be constructed using emission intensity of PNOH at 502 nm with two chemical inputs,  $\text{H}^+$  and  $\text{PO}_4^{3-}$  as Input-1 and Input-2. Here, the emission intensity at 502 nm is monitored as the output signal. Following the principle of AND and NOT binary logic function, truth table has been constructed at the molecular level. With these two chemical inputs PNOH acts as an

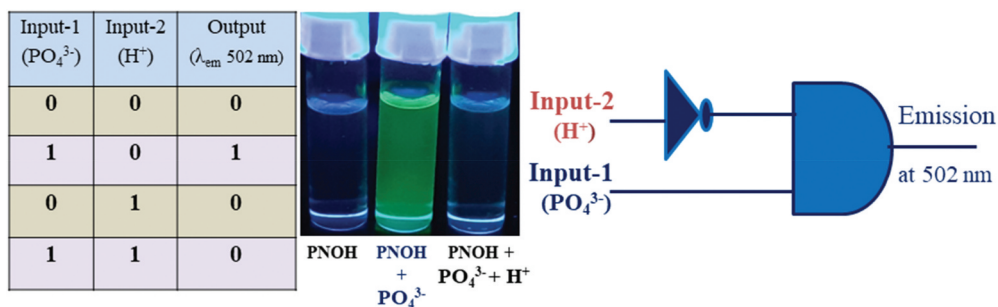


**Figure 6.** INHIBIT logic gate construction using  $\text{PO}_4^{3-}$  complex of PNOH with  $\text{H}^+$ . ( $\lambda_{\text{ex}} = 420 \text{ nm}$ ).

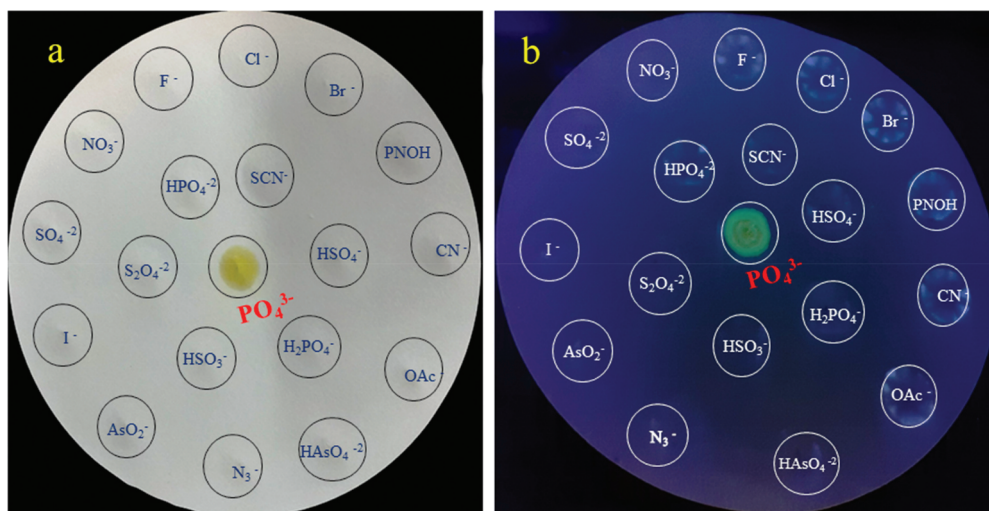


**Figure 7.** Photographs of paper strips study (a) in normal light (b) under 365-nm light irradiation.

AND gate with an inverter in the input-1 by monitoring the emission output. This function can be interpreted as a single molecular circuit showing an INHIBIT logic functions.

### 3.3. Paper strips study

To explore the practical application of sensor PNOH towards  $\text{PO}_4^{3-}$  ion, paper strips study was carried out. At first, paper strips of PNOH were prepared by placing a drop of PNOH ( $10^{-2}$  M) solution in DMSO on a filter paper and dried in air. Then, aqueous solution of each anion ( $10^{-2}$  M) was added drop wise onto each drop of PNOH. It is observed that only  $\text{PO}_4^{3-}$  ion makes a yellow colour spot in daylight and greenish-yellow under irradiation of 365 nm light (Figure 7) and other anions remain same as the probe. Therefore, test strip of sensor PNOH can be used to detect  $\text{PO}_4^{3-}$  anion in naked eye as well as under UV light.

### 3.4. Real sample study

Detection of analytes in real sample is an important criterion for any newly developed chemosensor. Hence, we have explored the sensing of PNOH towards  $\text{PO}_4^{3-}$  ion in real water samples. We have collected river water from 'Kangsabati river' situated nearly 2 km away from our campus and marked it as 'Sample-1'. Since many microorganisms and aquatic life are present in river, we may expect the presence of phosphate in river water. Solution of powder milk (bought from nearby retailer shop) is marked as Sample-2. Since phosphate-based fertiliser are used for cultivation, we collected water of paddy field (from nearby paddy field) and marked it as 'Sample-3'. We have checked the pH of all real sample solution in pH metre and it shows that the pH of all real sample solution is around 5–7. So, there is no involvement of  $\text{OH}^-$  ion towards  $\text{PO}_4^{3-}$  ion sensing. At first, we prepared  $10^{-2}$  (M) solution of  $\text{PO}_4^{3-}$  ion in double-distilled water. Then, a fixed (13.5  $\mu\text{l}$ ) amount of prepared  $\text{PO}_4^{3-}$  ion solution was spiked to 3 ml of each real sample. Stock

solution of PNOH (40  $\mu\text{M}$ ) was added to each real sample with spiked  $\text{PO}_4^{3-}$  ion (45  $\mu\text{M}$ ) separately and emission spectra were taken with  $\lambda_{\text{ex}} = 420 \text{ nm}$ . Our study shows that there is nearly 23%, 35% and 43% increase of emission intensity at 502 nm of sample-1, 2 and 3, respectively, compare to double-distilled water containing 45  $\mu\text{M}$   $\text{PO}_4^{3-}$  ion. Now subtracting the emission intensity at 502 nm due to spiked  $\text{PO}_4^{3-}$  ion, concentration of  $\text{PO}_4^{3-}$  ion are found to be 0.35, 0.78 and 0.95 ppm and percentage of recovery are 109, 120 and 126, respectively, as shown in the Table S2.

## 4. Conclusions

In conclusion, we have used our previously reported naphthalene-based probe 1-(Pyridin-2-yl-hydrazonomethyl)-naphthalen-2-ol (PNOH) and demonstrated its sensing ability towards  $\text{PO}_4^{3-}$  both colorimetrically and fluorometrically. Our UV-Vis,  $^1\text{H}$  NMR and steady-state and time resolved emission study show that the 'turn on' emission of PNOH in the presence of  $\text{PO}_4^{3-}$  arises from the excited PNO<sup>-</sup> ion. The probe PNOH shows high selectivity and sensitivity towards  $\text{PO}_4^{3-}$  ion with a limit of detection (LOD) of 0.35  $\mu\text{M}$ . In addition, a simple paper strip system has been developed using PNOH for the rapid monitoring of  $\text{PO}_4^{3-}$  in the real water samples. Again, the fluorescence 'turn-on' and 'turn-off' properties of PNOH in the presence of  $\text{PO}_4^{3-}$  and  $\text{H}^+$  has been demonstrated to construct molecular INHIBIT logic gate. We envisage that a simple one-step synthetic strategy and sensing mechanism reported in this work will smoothen the progress of the development of new colorimetric and fluorescent probe of  $\text{PO}_4^{3-}$  ion.

## Acknowledgments

N. Mudi (Award No.: 09/599(0075)/2018-EMR-I), S. S. Samanta (Award No.: 09/599(0084)/2019-EMR-I), P. K. Giri (Ref. No.: 228/(CSIR-UGC NET DEC 2017)) and U. Mandal (Ref. No.: 188/(CSIR-UGC NET JUNE 2019)) thank CSIR and UGC, New Delhi, India for their individual fellowship. Departmental instrumental facilities from DST FIST and UGC SAP programs are gratefully acknowledged. We also acknowledge the help render by USIC, Vidyasagar University for doing both steady-state and time resolved fluorescence study. We are thankful to the reviewers for their suggestion to explore the mechanism of sensing.

## Disclosure statement

No potential conflict of interest was reported by the author(s).

## Funding

The work was supported by the Council of Scientific and Industrial Research, India.

## References

- [1] U. Manna, S. Kayal, B. Nayaka and G. Das, Dalton Trans. **46**, 11956 (2017). doi:10.1039/C7DT02308A.
- [2] K. Bowman-James, A. Bianchi and E. Garca-Espaça, *Anion Coordination Chemistry* (Wiley-VCH, Weinheim, 2011). doi:10.1002/9783527639502.

- [3] R. Chelli, G. Pietraperzia, A. Bencini, C. Giorgi, V. Lippolis, P.R. Salvia and C. Gellini, *Phys. Chem. Chem. Phys.* **17**, 10813 (2015). doi:10.1039/C5CP00131E.
- [4] S.K. Dey, A. Basu, R. Chutiaa and G. Das, *RSC Adv.* **6**, 26568 (2016). doi:10.1039/C6RA00268D.
- [5] Q. Lin, T.T. Lu, X. Zhu, B. Sun, Q.P. Yang, T.B. Weia and Y.M. Zhang, *Chem. Commun.* **51**, 1635 (2015). doi:10.1039/C4CC07814D.
- [6] J.M. Mercurio, A. Caballero, J. Cookson and P.D. Beer, *RSC Adv.* **5**, 9298 (2015). doi:10.1039/C4RA15380D.
- [7] Y. Mikata, R. Ohnishi, R. Nishijima and H. Konno, *Inorg. Chem.* **55**, 11440 (2016). doi:10.1021/acs.inorgchem.6b01967.
- [8] M.K. Deliomeroglu, V.M. Lynch and J.L. Sessler, *Chem. Sci.* **7**, 3843 (2016). doi:10.1039/C6SC00015K.
- [9] Q.Y. Cao, T. Pradhan, S. Kim and J.S. Kim, *Org. Lett.* **13**, 4386 (2011). doi:10.1021/ol201722d.
- [10] M.R. Awwal, *J. Clean. Prod.* **228**, 1311 (2019). doi:10.1016/j.jclepro.2019.04.325.
- [11] Y. Ma, Y. Zhang, X. Li, P. Yang, J.Y. Yue, Y. Jiang and B. Tang, *Anal. Chem.* **92**, 3722 (2020). doi:10.1021/acs.analchem.9b04958.
- [12] X.J. Jiang, Y. Fu, L.H. Xu, H.L. Lu, S.Q. Zang, M.S. Tang and T.C.W. Ma, *Sens. Actuators B* **202**, 388 (2014). doi:10.1016/j.snb.2014.05.098.
- [13] D.Y. Kim, D.G. Kim, B. Jeong, Y.I. Kim, J. Heo and H.K. Lee, *Polymers* **14**, 190 (2022). doi:10.3390/polym14010190.
- [14] S.Q. Jiang, Z.Y. Zhou, S.P. Zhuo, G.G. Shan, L.B. Xing, H.N. Wanga and Z.M. Su, *Dalton Trans.* **44**, 20830 (2015). doi:10.1039/C5DT03814F.
- [15] I. Kaur, P. Kaur and K. Singh, *Sens. Actuators B Chem.* **257**, 1083 (2018). doi:10.1016/j.snb.2017.10.173.
- [16] Y.S. Zheng, Y.X. Yuan and J.H. Wang, *Chem. Asian J* **14**, 760 (2018). doi:10.1002/asia.201801585.
- [17] J. Zhao, D. Yang, Y. Zhao, X.J. Yang, Y.Y. Wang and B. Wu, *Angew. Chem.* **126**, 6750 (2014). doi:10.1002/ange.201402169.
- [18] N. Mudi, P. Hazra, M. Shyamal, S. Maity, P.K. Giri, S.S. Samanta, D. Mandal and A. Misra, *J. Fluoresc.* **31**, 315 (2021). doi:10.1007/s10895-020-02664-2.
- [19] E. Zeynaloo, E.M. Zahran, E.M. Fatila, A.H. Flood and L.G. Bachas, *Anal. Chem.* **93**, 5412 (2021). doi:10.1021/acs.analchem.0c04801.
- [20] M. Shyamal, P. Mazumdar, S. Maity, G.P. Sahoo, G. Salgado-Moran and A. Misra, *J. Phys. Chem. A* **120**, 210–220 (2016). doi:10.1021/acs.jpca.5b09107.
- [21] J.R. Lakowicz, *Principle of Fluorescence Spectroscopy* (Springer, New York, 2006). doi:10.1007/978-0-387-46312-4.
- [22] A.M. Brouwer, *Pure Appl. Chem.* **83**, 2213 (2011). doi:10.1351/PAC-REP-10-09-31.
- [23] A. SenGupta, K. Paula and V. Luxami, *Anal. Methods* **10**, 983 (2018). doi:10.1039/C7AY02779F.
- [24] A.P. de Silva, in *Supramolecular Chemistry: From Molecules to Nanomaterial*, edited by Jonathan W. Steed and Philip A. Gale (John Wiley & Sons Ltd., New York, 2012).
- [25] N. Agius and D.C. Magri, *New J. Chem.* **45**, 14360 (2021). doi:10.1039/D1NJ03045K.